

## Coupled-channel Dalitz plot analysis of $D^+ \rightarrow K^- \pi^+ \pi^+$ decay

---

**Satoshi X. Nakamura\***

*Department of Physics, Osaka University*

*E-mail: nakamura@kern.phys.sci.osaka-u.ac.jp*

We demonstrate that partial wave amplitudes extracted from  $D^+ \rightarrow K^- \pi^+ \pi^+$  Dalitz plot with a unitary coupled-channel model are significantly different from those obtained with an isobar model. The unitary coupled-channel model takes account of hadronic rescattering mechanisms involving all three mesons that have been missed in conventional isobar model analyses. The rescattering mechanisms contribute largely, and can triplicate the  $D^+ \rightarrow K^- \pi^+ \pi^+$  decay width within our analysis. These findings deliver a warning that analysis results obtained with isobar models should be looked with a caution. The determination of the CKM angle  $\gamma/\phi_3$  is a highly relevant problem.

*VIII International Workshop On Charm Physics*  
*5-9 September, 2016*  
*Bologna, Italy*

---

\*Speaker.

## 1. Introduction

Dalitz plots from heavy meson decays have been conventionally analyzed with isobar models. The model assumes, for example, a  $D$ -meson decays into an excited state  $R$  ( $\bar{K}, \bar{K}^*$ , etc.) and a pseudoscalar meson, and the  $R$  subsequently decays into a pair of pseudoscalar mesons; the third pseudoscalar meson is treated as a spectator [Fig. 1(left)]. The total decay amplitude is given by a coherent sum of these isobar amplitudes plus a flat background. Although the isobar models have been quite successful in getting precise fits to the data, this does not necessarily mean that a (partial wave) decay amplitude extracted with the model is the right one. This is because what the data can constrain is only the modulus of the total decay amplitude. Therefore, one should use a theoretically sound model for extracting amplitudes from the data so that unnecessary model artifact does not come into play. An obvious concern about the isobar model is that it misses mechanisms involving what we call Z-diagrams as shown in Fig. 1 (red dotted rectangle). The Z-diagrams must be considered to take care of full channel-couplings and the three-body unitarity.

In this contribution, we demonstrate that partial wave amplitudes extracted from  $D^+ \rightarrow K^- \pi^+ \pi^+$  Dalitz plot with an isobar model are significantly different from those obtained with a unitary coupled-channel model. We also show a large contribution from the three-body rescattering to the Dalitz plot distribution. Through these investigations, we address the validity of the isobar model in extracting decay amplitudes. A full account of this work is given in Ref. [1]. To the best of our knowledge, this is the first full Dalitz plot analysis of a  $D$ -meson decay into three pseudoscalar mesons with a coupled-channel framework. Findings here are also relevant to extracting the CKM angle  $\gamma/\phi_3$  from data of  $B^\pm \rightarrow \tilde{D}^0 h^\pm$  ( $\tilde{D}^0 = D^0$  or  $\bar{D}^0$ ;  $h = \pi, K$ , etc.) followed by  $\tilde{D}^0 \rightarrow 3$  mesons. In there, it is crucial to accurately determine the  $\tilde{D}^0$  decay amplitude and particularly its phase [2].

The three-body final state interaction in the  $D^+ \rightarrow K^- \pi^+ \pi^+$  decay was also studied and its importance was shown by other groups [3, 4]. The  $K^- \pi^+$   $s$ -wave amplitude from an experimental analysis was studied in Ref. [3]. Meanwhile, the elastic region of the  $D^+ \rightarrow K^- \pi^+ \pi^+$  decay Dalitz plot was analyzed with a dispersion theoretical framework in Ref. [4], and decay amplitudes were extracted.

In what follows, our coupled-channel model to describe the  $D^+ \rightarrow K^- \pi^+ \pi^+$  decay amplitude is discussed in Sec. 2. Then in Sec. 3, we present numerical results from our analyses of the two-pseudoscalar-meson scattering data, and of the  $D^+ \rightarrow K^- \pi^+ \pi^+$  decay Dalitz plot pseudo-data; the pseudo-data are generated with the E791 isobar model [5] and thus reasonably realistic.

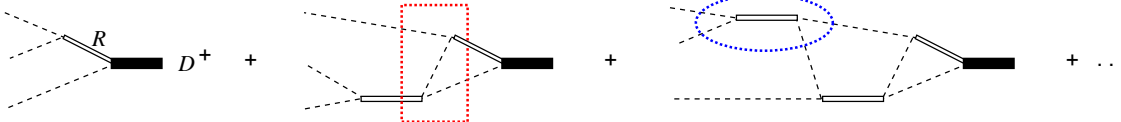


**Figure 1:** (Color online) Diagrammatic representation of  $D^+$ -decay into three pseudoscalar mesons in our coupled-channel model. The dashed lines represent propagations of pseudoscalar mesons. The part enclosed by the red dotted rectangle represents a Z-diagram, while the blue dotted ellipse cuts out an off-shell two-pseudoscalar-meson scattering amplitude. The leftmost diagram is an isobar diagram and the rest are rescattering diagrams involving the Z-diagrams.

## 2. Formulation

The unitary coupled-channel framework we work with here has been developed in our previous publications [6]. In this formalism,  $D^+$ -meson decays into a  $Rh$  channel ( $R$ : bare resonance), followed by multiple scatterings due to the hadronic dynamics, leading to the final  $K^- \pi^+ \pi^+$  state (Fig. 1); both the two-body and three-body unitarity are maintained. The main driving force for the hadronic rescattering is interactions between two pseudoscalar mesons. Therefore, we first construct a two-pseudoscalar-meson ( $\pi, K$ ) interaction model that is subsequently applied to three-pseudoscalar-meson scattering and then the  $D$  decay amplitude. The following presentations are also given in this order.

We describe two-pseudoscalar-meson scatterings with a unitary coupled-channel model. For example, we consider  $\pi\pi$ - $K\bar{K}$  coupled-channels for a  $\pi\pi$  scattering, while  $\pi\bar{K}$ - $\eta'\bar{K}$  coupled-channels for  $I=1/2$   $s$ -wave  $\pi\bar{K}$  scattering. We model the two-meson interactions with bare resonance( $R$ )-excitation mechanisms or contact interactions or both. These interactions are plugged in Lippmann-Schwinger equation that produces meson-meson scattering amplitudes.

For a three pseudoscalar-meson scattering, let us first assume that the three mesons interact with each other only through the above-described two-meson interactions. Because the two-meson interaction is given in a separable form, we can cast Faddeev equation into a two-body like scattering equation (the so-called Alt-Grassberger-Sandhas (AGS) equation [7]) for a  $\mathcal{R}h \rightarrow \mathcal{R}'h'$  scattering. Here,  $\mathcal{R}$  stands for either  $R$  or  $r_{ab}$ , and  $r_{ab}$  is a spurious “state” that is supposed to live within a contact interaction in a very short time, and decays into the two pseudoscalar-mesons,  $ab$ . The driving force for the scattering is the Z-diagrams [Fig. 1 (red dotted rectangle)] and the dressed  $\mathcal{R}$  propagators which include multiple insertions of self energy diagrams. In a three-meson system, there may be a room for a three-meson-force to play a role. The hidden local symmetry (HLS) model [8] can provide vector-meson exchange diagrams that work as a three-meson-force, and we consider them in our analysis of the  $D^+ \rightarrow K^- \pi^+ \pi^+$  decay to study their relevance.

Finally, the decay amplitude for  $D^+ \rightarrow K^- \pi^+ \pi^+$  in our coupled-channel model is diagrammatically represented in Fig. 1. The first term corresponds to the isobar contribution while the rests are the contribution from the hadronic rescattering described by the AGS equation.

## 3. Analysis results

Now we apply the coupled-channel formalism discussed in the previous section to analyses of data. First we determine the two-pseudoscalar-meson scattering model by analyzing  $\pi\bar{K}$  and  $\pi\pi$  scattering data. Then we analyze the  $D^+ \rightarrow K^- \pi^+ \pi^+$  decay Dalitz plot.

### 3.1 Two-pseudoscalar-meson scattering

We determine the model parameters of our  $\pi\pi$  and  $\pi\bar{K}$  scattering models by fitting empirical scattering amplitudes for  $E \lesssim 2$  GeV. This is the energy region relevant to the  $D^+ \rightarrow K^- \pi^+ \pi^+$  Dalitz plot analysis. These two-meson interaction models are a basic ingredient for describing the three-meson scattering in the  $D^+ \rightarrow K^- \pi^+ \pi^+$  decay.

We analyze the  $\pi\bar{K}$  scattering amplitudes from the LASS experiment [9] to determine the model parameters for  $\{L, I\} = \{0, 1/2\}, \{0, 3/2\}, \{1, 1/2\}, \{2, 1/2\}$  partial waves ( $L$ : total angular

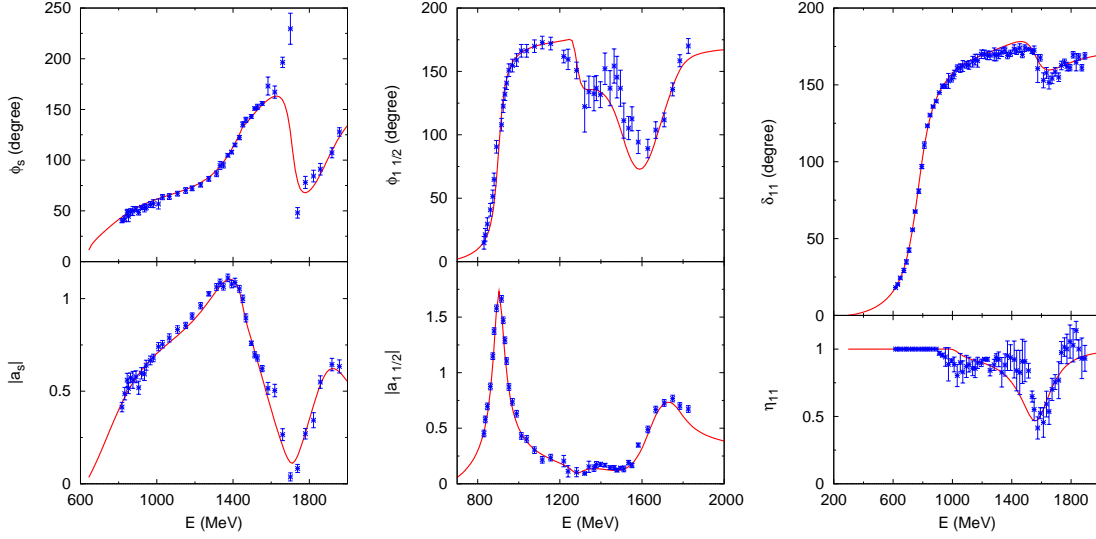


**Figure 2:** (Color online) Phase (upper) and modulus (lower) of the  $\pi\bar{K}$  scatterings amplitudes: (Left)  $L=0$  for  $\pi^+K^-$ ; (Center)  $\{L,I\}=\{1,1/2\}$ ; Data are from Ref. [9]. (Right) Phase-shifts and inelasticities for  $\{L,I\}=\{1,1\}$   $\pi\pi$  scattering. Data are from Ref. [10]. Figures taken from Ref. [1]. Copyright (2016) APS.

momentum;  $I$ : total isospin). For the  $\{L,I\}=\{0,1/2\}$  wave, we consider  $\pi\bar{K}-\eta'\bar{K}$  coupled channels. For the  $\{L,I\}=\{1,1/2\}$  and  $\{2,1/2\}$  waves, we consider coupling of  $\pi\bar{K}$  and effective inelastic channels. Regarding the  $\pi\pi$  model, the  $\{L,I\}=\{1,1\},\{0,2\}$  partial waves are needed for our coupled-channel analysis of the  $D^+ \rightarrow K^- \pi^+ \pi^+$  decay. We consider  $\pi\pi-K\bar{K}$  coupled channels for  $\{L,I\}=\{1,1\}$  and the elastic  $\pi\pi$  channel for  $\{L,I\}=\{0,2\}$ , and fit the CERN-Munich data [10].

We present the quality of the fits to the empirical amplitudes for the  $\pi^+K^- L=0$  and  $\{L,I\}=\{1,1/2\}$  partial waves in Fig. 2 (left, center) where phases (upper panels) and modulus (lower panels) of the amplitudes are shown. For the  $\pi\pi$  scattering, we present phase shifts and inelasticities for the  $\{L,I\}=\{1,1\}$  wave in Fig. 2 (right). As seen in the figure, the  $\pi\pi$  and  $\pi\bar{K}$  amplitudes our model generates are reasonable, and should be good enough for a coupled-channel analysis of the  $D^+ \rightarrow K^- \pi^+ \pi^+$ .

### 3.2 Analysis of $D^+ \rightarrow K^- \pi^+ \pi^+$ Dalitz plot

Now we perform a partial wave analysis of the  $D^+ \rightarrow K^- \pi^+ \pi^+$  Dalitz plot pseudo-data using our coupled-channel model. We explain setups of our models used in the analysis. In our coupled-channel framework,  $D^+$ -meson decays into  $\mathcal{R}h$  channels, and then hadronic rescatterings follows before a final  $K^- \pi^+ \pi^+$  state appears (Fig. 1). We consider the following 11  $\mathcal{R}h$  coupled channels in our full calculation:

$$\{\mathcal{R}h\} = \{R_1^{01}\pi, R_2^{01}\pi, r_{\pi\bar{K}}^{01}\pi, R_1^{11}\pi, R_2^{11}\pi, R_3^{11}\pi, R_1^{21}\pi, R_1^{12}\bar{K}, R_2^{12}\bar{K}, r_{\pi\bar{K}}^{03}\pi, r_{\pi\pi}^{04}\bar{K}\}, \quad (3.1)$$

where  $R_i^{L,2I}$  stands for  $i$ -th bare  $R$  state with the spin  $L$  and the isospin  $I$ ; when  $I$  is an integer (half-integer), it is understood that this  $R$  state has the strangeness  $S=0$  ( $S=-1$ ) in this report. Thus,  $R_1^{01}$ ,  $R_1^{11}$ ,  $R_2^{11}$ ,  $R_1^{12}$  are seeds of  $\bar{K}_0^*$ ,  $\bar{K}^*$ ,  $\bar{K}_2^*$ ,  $\rho$  resonances, respectively. In our model, these resonances are included as poles in the unitary scattering amplitudes. The  $\pi\pi$   $\{L,I\}=\{1,1\}$  partial

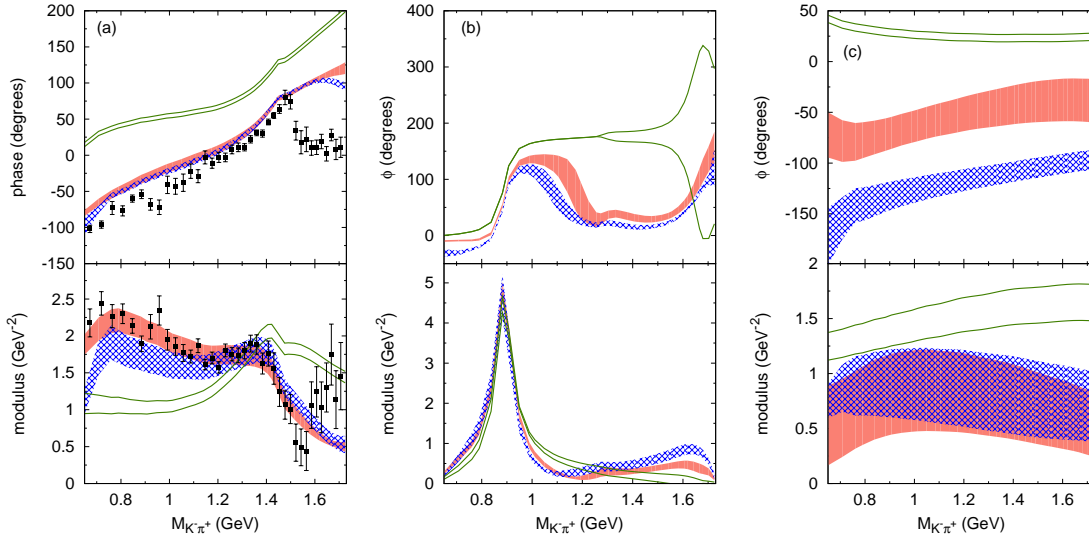


**Figure 3:** (Color online) Partial wave amplitudes extracted from the  $D^+ \rightarrow K^- \pi^+ \pi^+$  Dalitz plot. Phase (upper) and modulus (lower) are shown for (a)  $(K^- \pi^+)_S^{I=1/2} \pi^+$ ; (b)  $(K^- \pi^+)_P^{I=1/2} \pi^+$ ; (c)  $(K^- \pi^+)_S^{I=3/2} \pi^+$ . The red solid, blue cross-hatched, and green bordered bands are for the Full, Z, and Isobar models, respectively; the band widths represent the statistical errors. The  $(K^- \pi^+)_S \pi^+$  amplitude from the MIPWA of the E791 Collaboration [5] is shown by the black squares. Figures taken from Ref. [1]. Copyright (2016) APS.

wave associated with the  $R_i^{12} \bar{K}$  channel has not been considered in the previous isobar analyses of  $D^+ \rightarrow K^- \pi^+ \pi^+$ . This channel can contribute only through channel-couplings induced by the Z-diagrams, and therefore it does not show up in isobar models. We do not include a flat interfering background amplitude. We fit Dalitz plot pseudo-data for  $D^+ \rightarrow K^- \pi^+ \pi^+$  by adjusting parameters associated with the  $D^+ \rightarrow \mathcal{R}h$  vertices (couplings, phases).

In our analysis of  $D^+ \rightarrow K^- \pi^+ \pi^+$  Dalitz plot pseudo-data, three models are used. The first one is the “Full model” that contains all the dynamical contents described above. The second one is the “Z model” for which the rescattering mechanism is solely due to multiple iteration of the two-pseudoscalar-meson interactions in the form of the Z diagrams and  $\mathcal{R}$  propagators; no three-meson-force. The third model is the “Isobar model” that does not explicitly include the Z-diagrams. Finally we remark that the two-pseudoscalar-meson interactions will not be adjusted to fit the  $D^+$ -decay pseudo-data. This is in contrast with most of the previous analyses where some of Breit-Wigner parameters associated with  $R$ -propagations were also adjusted along with  $D^+ \rightarrow Rh$  vertices. After the fits, we obtained the Full, Z, and Isobar models for which  $\chi^2/\text{d.o.f.} = 0.22, 0.17,$  and  $0.42$ , respectively.

We present in Fig. 3 partial wave decay amplitudes extracted in the analysis; the horizontal axis is the invariant mass of  $K^- \pi^+$ ,  $M_{K^- \pi^+}$ . We denote a partial wave by “ $(ab)_L^I c$ ” in which a two-pseudoscalar-meson pair  $ab$  has the total angular momentum  $L$  and the total isospin  $I$ . The partial wave amplitudes for  $(K^- \pi^+)_S^{I=1/2} \pi^+$ ,  $(K^- \pi^+)_P^{I=1/2} \pi^+$ , and  $(K^- \pi^+)_S^{I=3/2} \pi^+$  are presented in Figs. 3(a)-(c), respectively. As a whole, the Full and Z models are similar in the amplitudes while the Isobar model is rather different, particularly in  $(K^- \pi^+)_S^{I=1/2} \pi^+$  and  $(K^- \pi^+)_S^{I=3/2} \pi^+$ . Because the models maintain the Watson theorem when the Z-diagrams are absent, the phases (the upper panels of Fig. 3) from the Isobar model in the elastic region are essentially the same as those

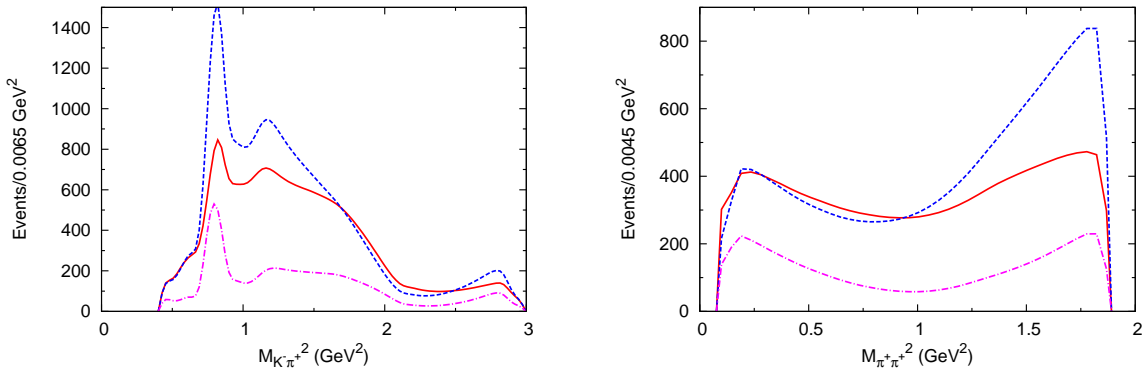


**Figure 4:** (Color online) The  $K^- \pi^+$  (left) and  $\pi^+ \pi^+$  (right) squared invariant mass spectrum for  $D^+ \rightarrow K^- \pi^+ \pi^+$ . The red solid curves are from the Full model. The blue dashed curves are also from the Full model but the three-meson-force is turned off. The magenta dot-dashed curves are from the Full model with all the rescattering involving the Z-diagrams turned off. Figures taken from Ref. [1]. Copyright (2016) APS.

of the LASS  $\pi \bar{K}$  amplitude up to overall constant shifts. The difference in the  $M_{K^- \pi^+}$ -dependence of the phases between the Isobar model and the Full (or Z) model is solely due to the effect of the hadronic rescattering involving the Z-diagrams.

In Fig. 3(a), we also show the  $(K^- \pi^+)_S \pi^+$  amplitude from the E791 MIPWA (model independent partial wave analysis) [5] denoted by  $[(K^- \pi^+)_S \pi^+]_{\text{MIPWA}}^{\text{E791}}$ . Interestingly, the  $M_{K^- \pi^+}$ -dependence of the phases from the Full and Z models are in a very good agreement with those of the MIPWA for  $M_{K^- \pi^+} \lesssim 1.5$  GeV. Thus, our coupled-channel models explain the difference between the phase of  $[(K^- \pi^+)_S \pi^+]_{\text{MIPWA}}^{\text{E791}}$  and that of the LASS  $(K^- \pi^+)_S^{I=1/2} \pi^+$  amplitude in a way qualitatively different from the previous explanation. Edera et al. [11] and the FOCUS  $K$ -matrix model analysis [12] explained the difference with a rather large (more than 100%) destructive interference between the  $(K^- \pi^+)_S^{I=1/2} \pi^+$  and  $(K^- \pi^+)_S^{I=3/2} \pi^+$  amplitudes, without an explicit consideration of the three-body hadronic rescattering. Our coupled-channel models, on the other hand, explained the difference with the hadronic rescattering involving the Z-diagrams, and have a moderately destructive interference between the  $(K^- \pi^+)_S^{I=1/2} \pi^+$  and  $(K^- \pi^+)_S^{I=3/2} \pi^+$  amplitudes.

We notice in Fig. 3(c) that the  $(K^- \pi^+)_S^{I=3/2} \pi^+$  partial wave amplitude has relatively large errors. Because we analyzed the data of the single charge state, it may be difficult to separate the different isospin states with a good precision. This situation would be improved by analyzing data of different charge states, i.e.,  $D^+ \rightarrow K^- \pi^+ \pi^+$  and  $D^+ \rightarrow K_S^0 \pi^+ \pi^0$ , in a combined manner.

Now let us study how much the three-meson-force contributes to the  $D^+ \rightarrow K^- \pi^+ \pi^+$  decay. In Fig. 4, we compare the  $K^- \pi^+$  ( $\pi^+ \pi^+$ ) squared invariant mass spectrum of the Full model with those from the same model but the three-meson-force being turned off. The three-meson-force suppresses the decay width by  $\sim 22\%$ , and change the spectrum shape significantly, as seen in Fig. 4. In the same figure, we also show the spectrum from the Full model with all the Z-diagrams (diagrams except for the first term in Fig. 1) being turned off. Effects of the Z-induced rescattering mechanisms are quite large; the decay width gets almost triplicated by the rescattering effect. In particular, we found that the hadronic rescattering through partial wave  $(\pi^+ \pi^0)_P^{I=1} \bar{K}^0$ , which includes  $\rho(770)$ , gives a major contribution.

#### 4. Summary and future perspective

The analysis conducted here clearly showed the importance of the hadronic rescattering involving the Z-diagrams that have been missed in the conventional isobar model analyses. Partial wave amplitudes extracted from Dalitz data with an isobar model should be looked with a caution.

For a further improved analysis, a combined analysis of related processes would greatly help. For example, by simultaneously analyzing the  $D^+ \rightarrow K^- \pi^+ \pi^+$  and  $D^+ \rightarrow K_S^0 \pi^0 \pi^+$  decays, the isospin separation of the amplitude would be better done. Also, we expect the role of  $\rho(770)$  in the decays to be extracted reliably, because the BESIII analysis [13] found its dominant contribution to  $D^+ \rightarrow K_S^0 \pi^0 \pi^+$ . We stress that combined analyses are very common for the baryon spectroscopy [14], and the coupled-channel unitarity is a guiding principle there. In the CHARM 2016 workshop, we heard three talks on  $D^+ \rightarrow K^- K^+ K^+$  Dalitz plot analysis [15, 16]. The experimental analysis found three comparable solutions for the  $K^- K^+$   $s$ -wave amplitude [15]. A combined analysis of  $D^+ \rightarrow K^- K^+ K^+$  and  $K^+ \pi^- \pi^+$  could discriminate one from the other solutions.

#### Acknowledgments

My participation to CHARM 2016 was supported by JSPS KAKENHI Grant Number JP25105010.

#### References

- [1] S.X. Nakamura, *Phys. Rev. D* **93** (2016) 014005.
- [2] A. Poluektov et al. (Belle Collaboration), *Phys. Rev. D* **81** (2010) 112002.
- [3] P.C. Magalhães et al., *Phys. Rev. D* **84** (2011) 094001;  
P.C. Magalhães and M.R. Robilotta, *Phys. Rev. D* **92** (2015) 094005.
- [4] F. Niecknig and B. Kubis, *JHEP* **1510** (2015) 142.
- [5] E.M. Aitala et al. (E791 Collaboration), *Phys. Rev. D* **73** (2006) 032004.
- [6] H. Kamano, S.X. Nakamura, T.-S.H. Lee, and T. Sato, *Phys. Rev. D* **84** (2011) 114019;  
S.X. Nakamura, H. Kamano, T.-S.H. Lee, and T. Sato, *Phys. Rev. D* **86** (2012) 114012.
- [7] E.O. Alt, P. Grassberger, and W. Sandhas, *Nucl. Phys. B* **2** (1967) 167.
- [8] M. Bando, T. Kugo, and K. Yamawaki, *Phys. Rept.* **164** (1988) 217.
- [9] D. Aston et al., *Nucl. Phys. B* **296** (1988) 493;  
P. Estabrooks et al., *Nucl. Phys. B* **133** (1978) 490.
- [10] B. Hyams et al., *Nucl. Phys. B* **64** (1973) 134.
- [11] L. Edera and M.R. Pennington, *Phys. Lett. B* **623** (2005) 55.
- [12] J.M. Link et al. (FOCUS Collaboration), *Phys. Lett. B* **653** (2007) 1.
- [13] M. Ablikim et al. (BESIII Collaboration), *Phys. Rev. D* **89** (2014) 052001.
- [14] H. Kamano, S.X. Nakamura, T.-S.H. Lee, and T. Sato, *Phys. Rev. C* **88** (2013) 035209.
- [15] A.C. dos Reis, *this proceedings*;  
T. Evans, *this proceedings*.
- [16] P.C. Magalhães, *this proceedings*;  
R.T. Aoude, P.C. Magalhães, A.C. dos Reis, and M.R. Robilotta, arXiv:1604.02904.